analytical chemistry

Subscriber access provided by UNIV OF CALIFORNIA SAN DIEGO LIBRARIES

Article

Dual microRNAs-fueled DNA nanogears: A case of regenerated strategy for multiple electrochemiluminescence detection of microRNAs with single luminophore

Pu Zhang, Ying Zhuo, Ruo Yuan, and Yaqin Chai

Anal. Chem., **Just Accepted Manuscript** • DOI: 10.1021/acs.analchem.6b04402 • Publication Date (Web): 19 Dec 2016

Downloaded from http://pubs.acs.org on December 20, 2016

Just Accepted

"Just Accepted" manuscripts have been peer-reviewed and accepted for publication. They are posted online prior to technical editing, formatting for publication and author proofing. The American Chemical Society provides "Just Accepted" as a free service to the research community to expedite the dissemination of scientific material as soon as possible after acceptance. "Just Accepted" manuscripts appear in full in PDF format accompanied by an HTML abstract. "Just Accepted" manuscripts have been fully peer reviewed, but should not be considered the official version of record. They are accessible to all readers and citable by the Digital Object Identifier (DOI®). "Just Accepted" is an optional service offered to authors. Therefore, the "Just Accepted" Web site may not include all articles that will be published in the journal. After a manuscript is technically edited and formatted, it will be removed from the "Just Accepted" Web site and published as an ASAP article. Note that technical editing may introduce minor changes to the manuscript text and/or graphics which could affect content, and all legal disclaimers and ethical guidelines that apply to the journal pertain. ACS cannot be held responsible for errors or consequences arising from the use of information contained in these "Just Accepted" manuscripts.

ACS Publications

Analytical Chemistry is published by the American Chemical Society. 1155 Sixteenth Street N.W., Washington, DC 20036

Published by American Chemical Society. Copyright © American Chemical Society. However, no copyright claim is made to original U.S. Government works, or works produced by employees of any Commonwealth realm Crown government in the course of their duties.

Dual microRNAs-fueled DNA nanogears: A case of regenerated strategy for multiple electrochemiluminescence detection of microRNAs with single luminophore

Pu Zhang, Ying Zhuo, Ruo Yuan*, Yaqin Chai*

Key Laboratory of Luminescent and Real-Time Analytical Chemistry (Southwest University), Ministry of Education, College of Chemistry and Chemical Engineering, Southwest University, Chongqing 400715, PR China

* Corresponding author. Tel.: +86-23-68252277; Fax: +86-23-68253172.

E-mail address: yuanruo@swu.edu.cn; yqchai@swu.edu.cn

ABSTRACT:

The determination of multiple biomarkers from cancer cells features a considerable step toward early diagnosis of cancers. However, realizing different biomarkers detection with single electrochemiluminescence (ECL) luminophore and regenerating the sensing platform remain a compelling goal. Herein, dual miRNAs-fueled DNA nanogears were designed for an enzyme-free ECL biosensor construction to perform the multiple sensitive detection of the microRNA (miRNA) biomarkers with single luminophore. The nanogears were assembled on CdS quantum dots (QDs) modified sensing surface. Using miRNA-21 as motive power, Au nanoparticles (AuNPs)-labeled nanogears B could be activated to roll against nanogear A, increasing the distance between AuNPs and CdS QDs. Thus the significant ECL enhancement of CdS QDs was obtained owing to the ECL energy transfer between AuNPs and CdS QDs, simultaneously realizing the detection of miRNA-21. After the incubation of miRNA-155, nanogear B revolved against nanogear A continuously and realized the close-range of AuNPs and CdS QDs, resulting in the quenching of ECL intensity due to the Förster energy transfer and realizing the analysis of miRNA-155. The successive locomotion of the nanogears led to a significant ECL increasing for analysis of miRNA-21 down to 0.16 fM and a remarkable ECL suppression for determination of miRNA-155 down to 0.33 fM. Impressively, the proposed biosensor was able to be regenerated along with the gears roll against each other. In general, this enzyme-free strategy initiates a new thought to realize the multiple ECL detection with single luminophore, paving the way for applications of nanomachines in

biosengsing and clinical diagnosis.

Keywords microRNA, DNA machine, regenerated biosensor, electrochemiluminescence

INTRODUCTION

As probably the most amazing molecule, DNA carries genetic information and serves as the central element of proliferation over billion years of the natural evolution.[1] Significantly, DNA has been widely identified to be a promising biomolecule for the assembly of novel nanostructures with specific performance and captured considerable attractions in recent years.[2,3] For instance, DNA-based artificial nanomachines and nanodevices are able to produce reversible, reasonable-designed nanometerscale motions, including "walkers", "spiders", "gears" and so on.[4,5] The majority of the existed machines in the real world are composed of "wheels" or "gears", rotating one against another with sufficient external stimulation. Tian and Mao demonstrated a couple of circular DNA molecule which could revolve against each other with rational design owing to the virtues of distinct base-pairing, static structures and flexibility of the DNA chains.[6] Despite the progress of the proposed nanogears, further application of the developed DNA nanogears in real samples has not been scientifically and systematically explored.

Small RNAs are defined according to the length (20-30 nucleotides) and the association with the Argonaute (AGO) family proteins, and they are divided into three categories: PIWI-interacting RNA (piRNA), microRNA (miRNA) and small interfering RNA (siRNA).[7,8] In recent years, the development of ageing is the key

causing factor for cardiovascular diseases and gives rise to an unfavorable result in patients. Surprisingly, miRNAs appear as predominant regulators of cardiovascular function and show considerable functions in diverse bio-processes.[9,10] Although advanced techniques for miRNA analysis have obtained impressive achievements, the sensing platform for miRNA detection must be reconstructed after it has been used, due to the loss of bioactivity of the biogenic elements or the damage caused to the sensor during the detection. [11-13] Regrettably, the reconstruction of the architecture asks for dozens of minutes or even a few days, which makes the application of the biosensors extravagant and inconvenient. Therefore, the progress of a generally regenerated sensing platform for miRNA analysis remains a realistic challenge. Fortunately, according to our knowledge, controlling the distance of the two DNA nanogears requires the complementary of the exposure strands of nanogears and the additional DNA/miRNA strands, making the miRNA as "fuel" to control the locomotion of the nanogears possible. Significantly, the above conception offers a guiding importance for the construction of a regenerated biosensor for miRNAs analysis with rational design.

In diverse strategies for the analysis of miRNA, electrochemiluminescence (ECL), as a powerful analysis tool, has been paid great attention owing to the low background response, easy operation and remarkable controllability.[14,15] Over the past few years, substantial efforts have been contributed to construct potential-resolved ECL for multiple targets determination because the emission of the luminescence from the luminophore was determined by potential.[16-18] It has been performed that

$Ru(bpy)_3^{2+}$ complex and $Ir(ppy)_3$ could emit ECL response under different potentials, achieving the multiple analysis with the two luminophores.[19,20] Furthermore, Jiang's group has offered an alternative platform for multiple antigens detection by applying $Ru(bpy)_3^{2+}$ and luminol as the ECL probes. In this way, the multiple detection by introducing two ECL luminophores as signal probe was achieved.[21] However, the above traditional strategies for multiple ECL detection cannot eliminate the cross-reaction of different ECL probes. More recently, our previous study has reported a multiparameter ECL analysis for multiple detection of biomarker proteins by multivariate linear algebraic equations based on introducing different ECL probes.[22] Although the multiparameter analysis has overcome the limitation from inevitable cross reactions, the above method asked for abundant laboratory data and required to establish complex mathematical model. In consequence, it is an urgent challenge to develop a feasible strategy, which is simple and able to overcome the cross-reaction of multiple luminophores for multiple ECL detection.

Inspired by the locomotion of the DNA nanogears, we intend to combine the dynamics of DNA nanogears and distance-based quenching and enhancement of ECL to realize the multiple detection of miRNA with single ECL probe. Herein, dual miRNAs-fueled DNA nanogears were introduced into an enzyme-free ECL biosensor to perform the multiple sensitive detection of the miRNA biomarkers. As shown in scheme 1, the prepared DNA nanogears (A and B) were composed of strand C and different DNA chains (A1, A2, A3 and Au nanoparticles (AuNPs)-labeled B1, B2, B3) respectively, which served as the locomotor gears in this work. Firstly, gear A was

incubated on the CdS quantum dots (QDs)-modified electrode, following by introducing nanogear B on the sensing platform with DNA hybridization of PtNPs-labeled L1 and A1, B1. Subsequently, L2 was introduced to hybridize with A2 and B2, realizing the stable structure of the nanogears system and quenching the ECL signal of CdS QDs owing to the double quenching effect that PtNPs and AuNPs were close contracted with CdS QDs simultaneously.[23,24] When miRNA-21 (target 1) was introduced to fully hybridize with L1, L1 was removed from the gear gradually. At the same time, significantly, AuNPs and CdS QDs were at a large separation and the ECL signal was enhanced by AuNPs owing to surface plasmon resonances from ECL energy transfer.[24] With rational design, gear B was brought much closer to the sensing surface after the hybridization of miRNA-155 (target 2), A3 and B3, resulting in the secondary ECL quenching. Subsequently, R2 was introduced to fully hybridize to L2, thus releasing L2 from the nanogear system. After that, L1 was employed to the sensing surface again to generate the "off" state of the sensor. After modified with R3, target 2 was released from A3 and B3, resulting in the regeneration of the proposed biosensor. With this skillful integration, the ECL signal switched along with the locomotion of the nanogear system. As a result, the proposed nanogear-based strategy exhibited a wide linear range from 50 pM to 0.5 fM of miRNA-21 and from 50 pM to 1 fM of miRNA-155, and a relatively low detection limit of 0.16 fM for miRNA-21 and 0.33 fM for miRNA-155. Furthermore, the proposed strategy could be employed to monitor miRNAs in cancer cells, demonstrating a significant potential of the sensor for early diagnosis of diseases. By integrating the the dynamics of DNA nanogears

and distance-based ECL energy transfer, this novel strategy realized the multiple detection of biomarkers with single ECL probe, avoiding the cross-reaction of different ECL probe. Significantly, thanks to the motility of the DNA nanomachine, the enzyme-free biosensor was convenient and stable enough to be regenerated with the gears rolling against each other, circumventing the complicated reconstruction process of the sensing platform. This work showed an initial step to construct nanogear system on the basis of a biosensor, realizing the multiple detection of miRNA with single ECL luminophore analysis. The successful application of the logical DNA nanogears demonstrated that those DNA nanomachines have the potential promising in accurate analyzing of different biomarkers for diagnosis of relevant cancers. By manually changing the target sequence and relating DNA sequences, various functional DNA moieties could be corporated into the DNA nanogears including other miRNAs, DNA, aptamers and bioimaging agents, making the nanogear system an ideal sensing candidate for the real applications.

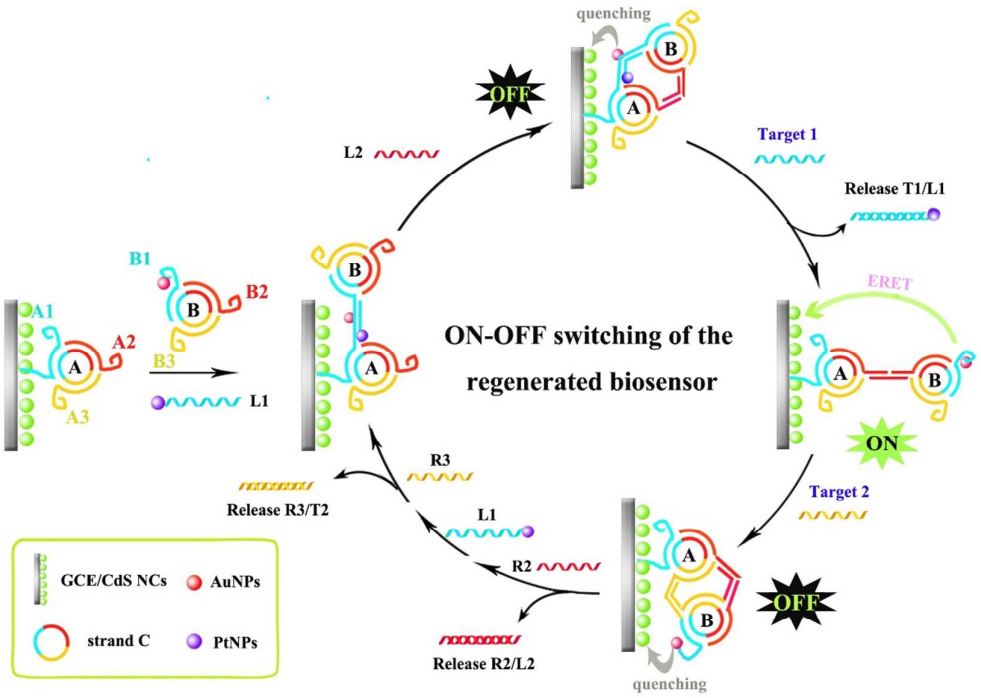

Scheme 1 The operating principle of the dual miRNAs-fueled nanogear-based regenerated biosensor which realized the multiple ECL detection of miRNAs with single luminophore.

EXPERIMENTAL SECTION

Reagents and apparatus. Potassium persulfate ($K_2S_2O_8$), cadmium nitrate tertrahydrate ($Cd(NO_3)_2{\cdot}4H_2O$) and sodium sulfide (Na_2S) were purchased from Shanghai Chemical Reagent Co. (Shanghai, China). Chlorauric acid ($HAuCl_4$), chloroplatinic acid (H_2PtCl_6), bovine serum albumin (BSA), mercaptoethanol (MCH), ethylene diamine tetraacetic acid (EDTA), citrate sodium, N-hydroxy succinimide (NHS) and N-(3-(Dimethylamino)propyl)-N′-ethylcarbodiimide hydrochloride (EDC) were obtained from Sigma-Aldrich (St. Louis, MO, U.S.A.). Oligonucleotides were custom-made by TaKaRa (Dalian, China) and Sangon (Shanghai, China). The oligonucleotides sequences are depicted in Table S1.

Phosphate-buffered solution (PBS) (pH 7.4, 0.1 M, including 0.1 M KCl, 0.1 M Na_2HPO_4 and 0.1 M KH_2PO_4) was used to dilute $K_2S_2O_8$. $[Fe(CN)_6]^{3-/4-}$ solution was set out using 10 mM $K_3Fe(CN)_6$, 10 mM $K_4Fe(CN)_6$, 0.1 M KCl, 0.1 M Na_2HPO_4 and 0.1 M KH_2PO_4. All the DNA strands were dissolved with TAE/Mg^{2+} buffer (pH 8.0, containing 2 mM EDTA, 40 mM Tris, 12.5 mM $Mg(Ac)_2$ and 20 mM CH_3COOH). MiRNAs used in this study were dissolved with miRNA hybridization buffer (pH 8.0, 1.0 mM EDTA, 10 mM $MgCl_2$, 0.2 M NaCl, 10 mM Tris-HCl,). Doubly distilled water was introduced throughout the study.

Cyclic voltammetric (CV) detections were performed with a CHI 660E electrochemistry workstation (Shanghai CH Instruments, China). ECL analysis were performed on a MPI-E ECL analyzer (Xi'an Remax Electronic Science & Technology Co). Transmission electron micrograph (TEM) screenages were achieved with a Tecnai G2 F20 microscope (FEI Co., U.S.A). All detections were put in a three-electrode system with the modified glassy carbon electrode (GCE) as the working electrode, Ag/AgCl (sat. KCl) as the reference electrode and platinum wire as the counter one. Besides, the voltage of the photomultiplier tube (PMT) was set at 800 V, the potential scanning ranged from -1.6 to 0.2 V.

Preparation of CdS QDs. CdS QDs used in this study were synthesized on the basis of a previously reported way.[24] Firstly, 0.1683 g of $Cd(NO_3)_2{\cdot}4H_2O$ was diluted in 30 mL ultrapure water and heated to 70 ºC under stirring. Then a solution of Na_2S (0.085 M) was added to the above solution and orange-yellow precipitates were observed instantly. The mixed solution was refluxed at 70 ºC for 3 h. The final product was

centrifuged and washed thoroughly with absolute ethanol and ultrapure water to get rid of the needless reagents. The proposed CdS QDs was characterized by TEM in supporting information (Fig. S1).

Preparation of AuNPs and PtNPs. AuNPs were prepared according to previous reports.[24] Briefly, 0.6 mL freshly prepared ice cold $NaBH_4$ (0.1 M) was joined to 20 mL aqueous solution containing 2.5×10^{-4} M $HAuCl_4$ under stirring. After that, the solution turned to orange-red color immediately.

The preparation of PtNPs was shown as follows:[23] 1 mL of 1 % H_2PtCl_6 was mixed with 100 mL ultra-pure water and heated to boiling. After that, 3 mL of 1% citrate sodium was joined into the above aqueous solution, followed by boiling the solution for 30 min. The obtained solution cooled down to 25 ºC with the obtained black colloidal solutions.

Preparation of L1-PtNPs and B1-AuNPs. 50 μL of 2 μM L1 was pretreated by 2 μL TCEP to avoid the formation of S-S bond. Afterwards, the activated DNA was employed into 5 mL of colloidal PtNPs. The mixture was kept at 4 ºC for 12 h to make sure the successful formation of Pt-S bond. Afterwards, 2% of BSA was introduced to the above mixture to block the nonspecific sites of PtNPs. At last, the obtained solution was centrifuged and washed with PBS twice, then resuspended in 1 mL of PBS and kept at 4 ºC for further use.

The synthesis of B1-AuNPs was indicated as follows: 50 μL of B1 (2 μM) was added into 500 μL AuNPs solution, followed by addition of 5 μL of 0.1 M MCH to improve the hybridization efficiency. The solution of B1-AuNPs was obtained after

being kept in 4 ºC for 2 h. At last, the obtained solution was centrifuged and washed with PBS twice, then resuspended in 1 mL of PBS and kept at 4 ºC for further use.

Preparation of gear A and gear B

Firstly, 2 μM of strand A1/B1 was added in 2 μM of strand C and heated to 95 ºC, then was permitted to cool down to 22 ºC over 1 h. Then 0.2 U of T4 ligase was incubated at 22 ºC for 16 h to link strand C into a circle. Subsequently, A2, A3/B2, B3 were introduced in the above solution and the proposed nanogears (circle A and circle B) were developed by slowly cooling the DNA mixture as follows: 95 ˚C (3 min), 65 ˚C (30 min), 50 ˚C (30 min), 37 ˚C (30 min) and 22 ˚C (30 min).

The determination of the designed miRNA sensor

Glassy carbon electrode (GCE, Φ = 4 mm) was attentively polished with 0.3 and 0.05 μm alumina powder on a polishing cloth respectively, achieving a mirror-like surface. The prepared GCE was firstly modified with CdS QDs with 12 h at room temperature to obtain a CdS QDs film on the surface of the electrode. Then gear A was modified on the electrode surface through Cd-S bond for 16h. Additionally, the sensing surface was modified with MCH for 40 min to block the nonspecific sites. Afterwards, gear B and L1-PtNPs were immobilized on the electrode, forming the nanogear system. Then the biosensor was further incubated with L2, miRNA-21 (target 1) and miRNA-155 (target 2) for 30 min gradually. Eventually, the proposed electrode was subsequently modified with R2, L1 and R3 for 30 min to reach the regeneration of the biosensor.

RESULTS AND DISCUSSION

Investigation of the nanogears. The proposed nanogears were characterized by Polyacrylamide gel electrophoresis (PAGE). The PAGE operating was showed in supporting information. As depicted in Figure 1, lane 3 corresponded to strand C which had been linked into a circle. After the addition of A1 and B1, strand A1 (lane 2: C+A1) and B1 (lane 4: C+B1) hybridized with strand C respectively. It can be observed that lane 2 posed a higher position because A1 had a larger molecular weight comparing with B1. Further incubation of A2, A3 and B2, B3 leaded to the formation of nanogear A (lane 1: C+A1+A2+A3) and nanogear B (lane 5: C+B1+B2+B3) with lower mobility, suggesting the gears were stable nanostructures. The rolling process was further investigated by PAGE (Figure 2). As expected, the proposed bands showed two different conformations. The two nanogears (A and B) which were linked by one DNA strand have a lower molecular weight (lane 1, 3, 5, 7). When the two nanogears were linked with two strands, the bands exhibited a slow mobility with higher molecular weight (lane 2, 4, 6). This result demonstrated that the rolling process of the nanogears were reasonable and practicable.

Figure 1. Formation of individual gears characterized by PAGE. lane 1: C+A1+A2+A3 (nanogear A); lane 2: C+A1; lane 3: strand C; lane 4: C+B1 and lane 5: C+B1+B2+B3 (nanogear B).

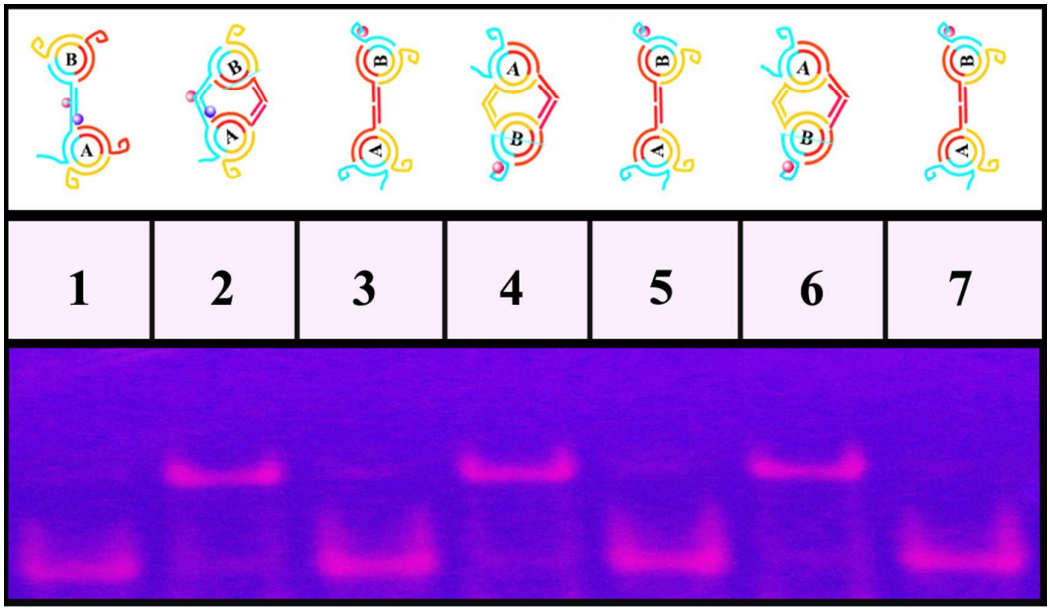

Figure 2. Characterization of the proposed rolling process of the nanogears. Lane 1: A+B+L1; lane 2: A+B+L1+L2; lane 3: A+B+L2; lane 4: A+B+L2+target 2; lane 5: A+B+target 2; lane 6: A+B +target 2+L1; lane 7: A+B+L1.

Electrochemical and ECL performance of the designed biosensor. To evaluate the electrochemical behavior of biosensor, CVs were measured in 5.0 mM $[Fe(CN)_6]^{3-/4-}$. As depicted in Figure 3A, a current signal of CV was observed on bare GCE (curve a). When CdS QDs were incubated on the sensing surface, the peak current decreased obviously due to the semiconductor properties of QDs (curve b). The current further decreased when incubated with gear A due to the electron hindrance of DNA chains (curve c). At last, the CV curve increased under the introduction of gear B (labled with AuNPs), L1 (labled with PtNPs) and L2, because AuNPs and PtNPs could

promote the electron transfer significantly (curve d).

Figure 3B summarized the ECL performance of our biosensor. As can be seen from the image, barely no ECL response was obtained on a bare electrode (curve a). When the electrode was modified with CdS QDs, a significant ECL response was achieved due to the introduction of ECL luminophore (curve b). When gear A was modified on the electrode, ECL intensity reduced because of the electron hindrance of DNA (curve c). After the incubation of gear B and L1, the ECL intensity decreased remarkably, because AuNPs can quench the ECL intensity of QDs at a close contact (curve d). The ECL signal further descended due to the quench property of L2-PtNPs towards QDs (curve e). Subsequently, when the biosensor switched to "on" state by the addition of target 1 (curve f), the ECL enhancement was produced due to the large separation of AuNPs and CdS. However, the proposed biosensor switched to the "off" state after modifying target 2 (curve g) with the proximity of AuNPs and CdS QDs. Finally, the surface of electrode was incubated with R2, L1 and R3, achieving the regeneration of the biosensor (curve h).

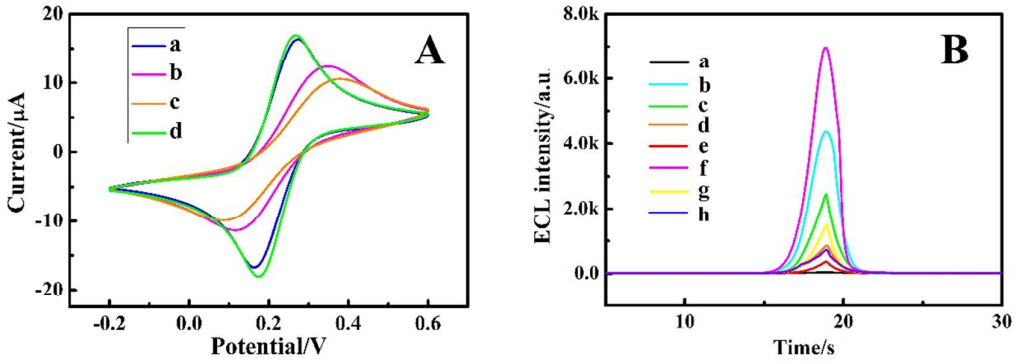

Figure 3. The electrochemical performance of the proposed biosensor (A): bare GCE (a), CdS/GCE (b), gear A/CdS/GCE (c), L2/L1/gear B/gear A/CdS/GCE (d). The ECL

characterization of the biosensor (B): bare GCE (a), CdS/GCE (b), gear A/CdS/GCE (c), L1/gear B/gear A/CdS/GCE (d), L2/L1/gear B/gear A/CdS/GCE (e), target 1/L2/L1/gear B/gear A/CdS/GCE (f), target 2/ target 1/L2/L1/gear B/gear A/CdS/GCE (g), R2, L1 and R3/target 2/ target 1/L2/L1/gear B/gear A/CdS/GCE (h), the potential scanning ranged from -1.6 to 0.2 V.

Analytical optimization of the proposed biosensor. In order to optimize the analytical sensing performance of the proposed biosensor, the incubation temperature and time of T4 ligase were investigated as showed in Figure S2 of the supporting information.

Significantly, since the energy transfer occurred based on distance of the luminophores, the suitable length between AuNPs and the CdS QDs was another vital factor that influence the enhancement efficiency and the sensitivity of the sensor. In consequence, the size of the gears was also studied. As Figure 4 described, curve a was achieved by incubating of 39-bases gears. When the biosensor was modified with 45-bases gears (curve b), the ECL intensity caused by target 1 increased obviously. The ECL intensity reached a maximum value when incubated with 53-bases gears (curve c). Thus, 53-bases gear was employed to detect the sensitivity of the proposed biosensor.

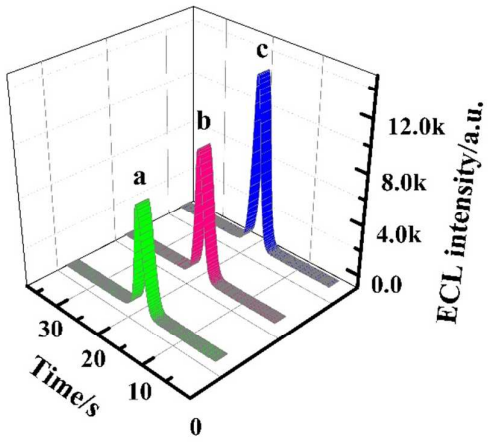

Figure 4. The relationship between ECL intensity and the size of the gears: (a) 39-bases gears; (b) 45-bases gears; (c) 53-bases gears, the potential scanning ranged from -1.6 to 0.2 V.

Measurement of multiple targets with the elaborate biosensor. The dependence of the ECL signal upon different concentrations of the two targets was determined under optimized conditions. As can be figured out from Figure 5A, the ECL response of the proposed biosensor increased gradually with incremental concentration of target 1 from 0.5 fM to 50 pM (curve a to f) and showed an advisable positive correlation with the logarithm of concentration with a linear equation of I = 10980.0 + 3081.2 lg c and a squared correlation coefficient of 0.992. The estimated detection limit of target 1 was 0.16 fM. However, it is clearly shown in Figure 5B that the incubation of different concentrations of target 2 (from 1 fM to 50 pM, curve a to f) to the sensing platform leaded to prominent decrease in ECL response under the saturated concentration of target 1. The detection limit of the target 2 was 0.33 fM. Furthermore, the linear equation was I = 6674.6 - 2792.8 lg c with the squared correlation coefficient of 0.991, where I represented the ECL response and c represented the

concentration of the two miRNAs. Furthermore, we have made a comparison of the proposed biosensor with the other detection strategy. As can be seen from Table 1, it can be figured out that the biosensor in this work has a relative lower detection limit and might have the potential of applying highly sensitive analysis in clinical bioassay.

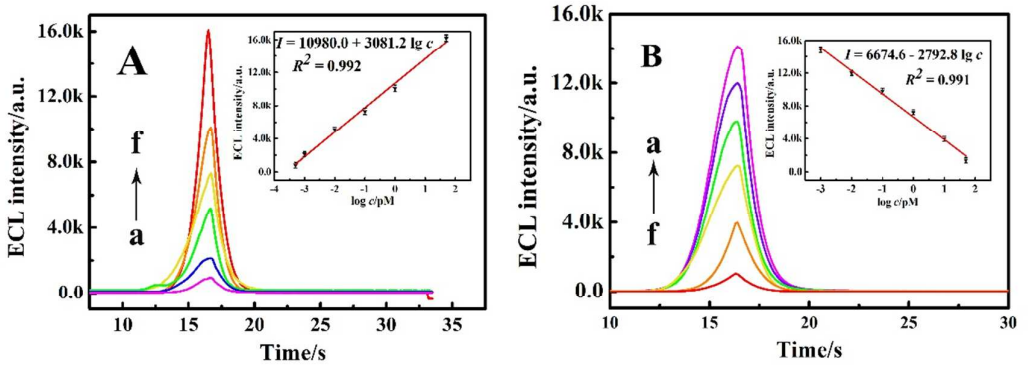

Figure 5. (A) ECL response of the elaborated biosensor in different concentrations of miRNA for detection of target 1: (a) 0.5 fM, (b) 1 fM, (c) 0.01 pM, (d) 0.1 pM, (e) 1 pM, (f) 50 pM. (B) ECL intensity of the biosensor in various concentrations of miRNA for detection of target 2: (a) 50 pM, (b) 10 pM, (c) 1 pM, (d) 0.1 pM, (e) 0.01 pM, (f) 1 fM, the potential scanning ranged from -1.6 to 0.2 V.

Table 1. The comparison of the proposed biosensor with other detection strategy

method	target	detection limit	references
fluorescent	miRNA	1 fM	25
fluorescent	miRNA	10 fM	26
fluorescent	miRNA	1 pM	27
ECL	miRNA	6.3 fM	28
ECL	miRNA	10 fM	29

Colorimetric	miRNA	2 nM	30
ECL	miRNA	0.16 fM/0.33fM	This work

Selectivity, stability and reproducibility of the miRNA biosensor. To investigate the selectivity of the prepared biosensor, miRNA-141, miRNA-182-5p and mismatched RNA for each target were chosen as the interfering agents. As seen from Figure 6A, the comparative detections were explored by using miRNA-141 (500 pM), miRNA-182-5p (500 pM), and mismatched RNA for miRNA-21 (500 pM) to replace miRNA-21 (50 pM), respectively. As expected, there were low ECL response on the interfering agents, while the tested target 1 (miRNA-21) and the mixture within miRNA-21 at a low concentration (50 pM) showed a significant ECL intensity. When analyzed target 2 (miRNA-155) and the mixture containing miRNA-155 at 50 pM, the ECL intensity showed unconspicuous signal compared to the interfering agents (500 pM) as depicted in Figure 6B. These results indicated that the proposed biosensor exhibited outstanding specificity as our expectation.

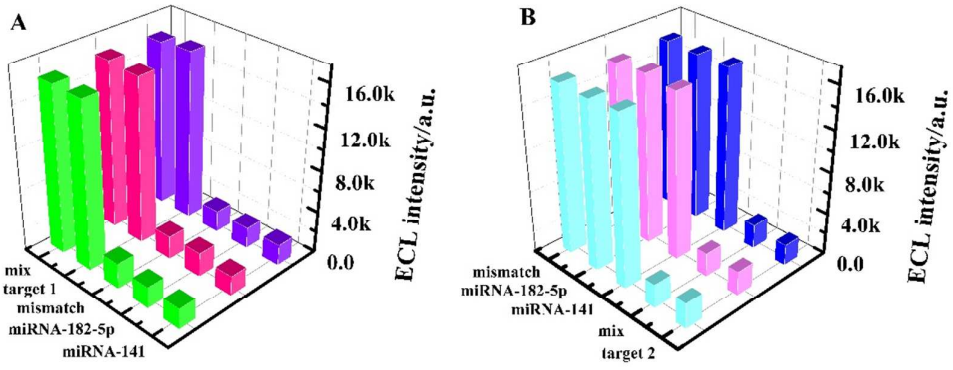

Figure 6. Comparison of ECL intensity with different targets: (A) miRNA-141 (500 pM), miRNA-182-5p (500 pM), mismatched RNA for miRNA-21 (500 pM), miRNA-21 (50 pM) and the mixture containing miRNA-21; (B) miRNA-141 (500

pM), miRNA-182-5p (500 pM), mismatched RNA for miRNA-155 (500 pM), miRNA-155 (50 pM) and the mixture containing miRNA-155.

Stability is another significant factor to estimate the performance of the proposed biosensor. As can be seen from Figure 7, the stability was estimated under continuous cyclic potential scans when the biosensor was modified with 50 pM of target 1. The image showed that the proposed biosensor had an excellent stability for 20 cycles.

To further study the reproducibility of the designed biosensor, intra- and inter-assays were explored. As showed in Figure S3, the RSD values of intra- and inter-assays by the variation coefficients were less than 5% for multiple duplicate experiments, respectively, suggesting the remarkable reproducibility of the ECL biosensor.

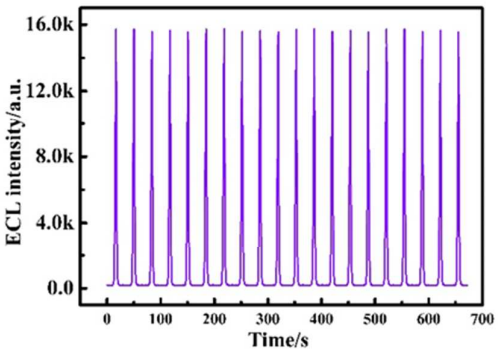

Figure 7. ECL stability of the elaborate biosensor under continuous cyclic potential scans for 20 cycles, the potential scanning ranged from -1.6 to 0.2 V.

Regenerability. To regenerate the biosensor, R2 was introduced to fully hybridize to L2, thus releasing L2 from the nanogear system. After that, L1 was employed to the sensing surface again to generate the "off" state of the sensor. After modified with R3, target 2 was released from A3 and B3, resulting in the regeneration of the proposed

biosensor. As can be depicted in Figure 8A, compared with the original "off" state (curve a), the ECL signal increased significantly after hybridizing with miRNA-21 (curve b). After a succession of the strand displacement of DNA chains, the sensor regenerated with a suppressed ECL signal of 98.3% (curve c). Furthermore, the proposed biosensor could be reproduced over three cycles for the analysis of two different miRNA targets (Figure 8B). This result demonstrated that the proposed biosensor possessed desirable regenerability, representing another attractive advantages of the sensing system.

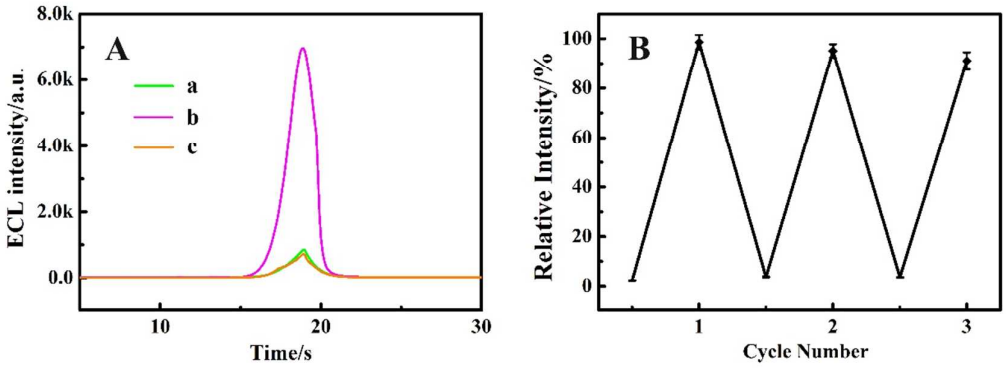

Figure 8. (A) ECL intensity of the regenerated sensor: the "off" state of the sensor (curve a); "on" state of the sensor (curve b); regeneration of the sensor with the representing of "off" state (curve c), the potential scanning ranged from -1.6 to 0.2 V. (B) The ECL response for miRNA detection over three cycles. The top dots represented the ECL signal of "on" state, whereas the bottom dots represented the ECL signal of "off" state.

Application. The applicability of proposed biosensor to practical samples is another important indicator in the development of miRNA analysis. Thus, the sensor was determined by detecting the above two miRNAs in the lysates from different cancer

cells. The cell culture was showed in the supporting information. As can be figured out in Figure 9A, bar b showed a slighter ECL response of miRNA from 100 cervical (Hela) cancer cells which was similar to the blank one (a). As expected, a further increase to 10^4 in Hela cells results in an inconspicuous increase in ECL intensity (d), suggesting that the miRNA-21 expressed in an especially low level in Hela cells. However, the positive result from human breast (MCF-7) cancer cells showed a significant increase in ECL intensity along with the increasing of the cell number, suggesting the overexpression of miRNA-21 in MCF-7 cells which showed good agreement with the published reports.[31]

Accordingly, the application to real cancer cell lysates of miRNA-155 was also investigated. In order to assure the accuracy of the miRNA-155 analysis, we introduced the saturated complementary strands of miRNA-21 in advance. As shown in Figure 9B, the lysate from Hela cells depicted a significant ECL response (b) which was in accordance with the blank detection (a). While the ECL intensity decreased from MCF-7 with the increasing of the cell number (c, d). The above consequence showed that miRNA-155 was overexpressed in MCF-7 instead of Hela, which was according with the previous work.[32, 33] With the favorable application of the proposed biosensor, we offered a feasible and prospect strategy for miRNAs detection with skillful DNA nanotechnology.

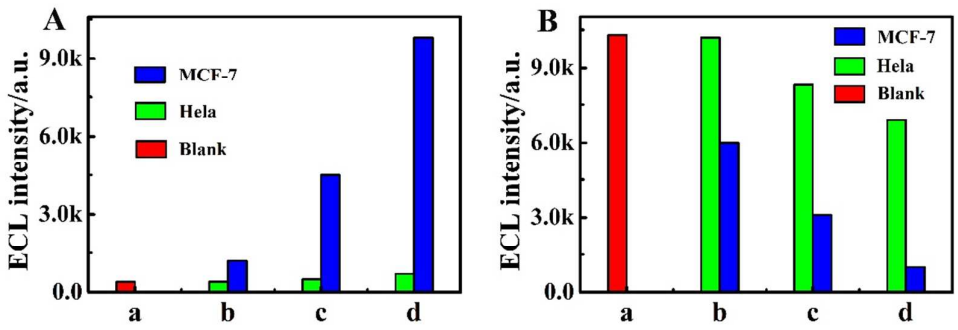

Figure 9. Analysis of miRNA-21 (A) and miRNA-155 (B) from MCF-7 and Hela cells: (a) blank detection without miRNAs; (b) 100 cancer cells; (c) 10^3 cancer cells; (d) 10^4 cancer cells.

CONCLUSIONS

In this paper, we have reported a dual miRNAs-fueled DNA nanogears based enzyme-free ECL biosensor for the ultrasensitive detection of multiple miRNA biomarkers. On the basis of the distance-based ECL emission, two DNA nanogears rolled against each other to reach the detection status which was powered by two miRNA biomarkers, enforcing the determination of two different miRNAs with single ECL probe. Compared with the traditional multiplexed ECL assay with more than one ECL probes, the proposed strategy avoided the limitation and complicity of the luminescence overlapping with different ECL probes. With the avoiding of any enzymes, the proposed biosensor led to a relative high sensitivity and could monitor miRNAs expression levels in cancer cells. Significantly, the proposed biosensor not only provides an efficient scheme for the multiple detection of miRNA biomarkers, but also realizes the regeneration of the sensor. This study demonstrated the fascination of DNA nanomachines when integrated with distance-based ECL response and the positive analysis may outline a significant scheme toward the development of

improved DNA artificial nanotechnology in the application of sensing, biomedicine and clinical diagnosis.

ASSOCIATED CONTENT

Supporting Information

Brief statement in nonsentence format listing the contents of the material supplied as Supporting Information.

AUTHOR INFORMATION

*Tel.: +86-23-68252277;

Fax: +86-23-68253172.

E-mail address: yuanruo@swu.edu.cn (R. Yuan), yqchai@swu.edu.cn (Y. Q. Chai)

Notes

The authors declare no competing financial interest.

ACKNOWLEDGEMENTS

This paper was financially supported by the National Natural Science Foundation of China (51473136, 21575116 and 21675129) and the Fundamental Research Funds for the Central Universities (XDJK2016E055), China.

REFRENCES

1 Winfree, E.; Liu, F.; Wenzler, L. A.; Seeman, N. C. *Nature*, 1998, **394**, 539-544.

2 Young, H. R.; Ruiz, Roanna C. H.; Peng, S. M.; Lee, J. B.; Luo, D. *Chem. Soc. Rev.*, 2011, **40**, 5730-5744.

3 Ranallo, S.; Amodio, A.; Idili, A.; Porchetta, A.; Ricci, F. *Chem. Sci.*, 2016, **7**, 66-71.

4 Zhang, F.; Nangreave, J.; Liu, Y.; Yan, H. *J. Am. Chem. Soc.*, 2014, **136**, 11198-11211.

5 Wang, Z. G.; Elbaz, J.; Willner, I. *Nano Lett.*, 2011, **11**, 304-309.

6 Tian, Y.; Mao, C. D. *J. Am. Chem. Soc.,* 2004, **126**, 11410-11411.

7 Tu, W. W.; Cao, H. J.; Zhang, L.; Bao, J. C.; Liu, X. H.; Da, Z. H. *Anal. Chem.*, 2016, **88**, 10459-10465.

8 Selbach, M.; Schwanhaeusser, B.; Thierfelder, N.; Fang, Z.; Khanin, R.; Rajewsky, N. *Nature*, 2008, **455**, 58-63.

9 Chan, A.; Krichevsky A. M.; Kosik, K. S. *Cancer Res.*, 2005, **65**, 6029-6033.

10 Qian, R. C.; Cao, Y.; Long, Y. T. *Anal. Chem.*, 2016, 88, 8640-8647.

11 Zhang, X. B.; Liu, C. H.; Sun, L. B.; Duana, X. R.; Li, Z. P. *Chem. Sci.*, 2015, **6**, 6213-6218.

12 Wang, L. D.; Deng, R. J.; Li, J. H. *Chem. Sci.,* 2015, **6**, 6777-6782.

13 Zhang, P.; Zhuo, Y.; Chang, Y. Y.; Yuan, R.; Chai, Y. Q. *Anal. Chem.*, 2015, **87**, 10385-10391.

14 Gao, W. Y.; Liu, Z. Y.; Qi, L. M.; Lai, J. P.; Kitte, S. A.; Xu, G. B. *Anal. Chem.*, 2016, **88**, 7654-7659.

15 Shi, H. W.; Zhao, W.; Liu, Z.; Liu, X. C.; Xu, J. J.; Chen, H. Y. *Anal. Chem.*, 2016, **88**, 8795-8801.

16 Deiss, F.; LaFratta, C. N.; Symer, M.; Blicharz, T. M.; Sojic, N.; Walt, D. R. *J. Am. Chem. Soc.,* 2009, **131**, 6088-6089.

17 Tian, D. Y.; Duan, C. F.; Wang, W.; Cui, H. *Biosens. Bioelectron.,* 2010, **25**,

2290-2295.

18 Chen, Z. H.; Liu, Y.; Wang, Y. Z.; Zhao, X.; Li, J. H. *Anal. Chem.,* 2013, **85**, 4431-4438.

19 Doeven, E. H.; Zammit, E. M.; Barbante, G. J.; Francis, P. S.; Barnett, N. W.; Hogan, C. F. *Chem. Sci.,* 2013, **4**, 977-982.

20 Doeven, E. H.; Barbante, G. J.; Kerr, E. C.; Hogan, F. J.; Endler, A.; Francis, P. S. *Anal. Chem.*, 2014, **86**, 2727-2732.

21 Han, F. F.; Jiang, H.; Fang, D. J.; Jiang, D. C. *Anal. Chem.*, 2014, **86**, 6896-6902.

22 Liang, W. B.; Fan, C. C.; Zhuo, Y.; Zheng, Y. N.; Xiong, C. Y.; Chai, Y. Q.; Yuan, R. *Anal. Chem.*, 2016, **88**, 4940-4948.

23 Zhang, H. R.; Xu, J. J.; Chen, H. Y. *Anal. Chem.*, 2013, **85**, 5321-5325.

24 Shan, Y.; Xu, J. J.; Chen, H. Y. *Chem. Commun.*, 2009, **8**, 905-907.

25 Yin, B. C.; Liu, Y. Q. Ye, B. C. *Anal. Chem.*, 2013, **85**, 11487-11493.

26 Duan, R. X.; Zuo, X. L.; Wang, S. T.; Quan, X. Y.; Chen, D. L.; Chen, Z. F.; Jiang, L.; Fan, C. H.; Xia, F. *J. Am. Chem. Soc.*, 2013, **135**, 4604-4607.

27 Xu, F. Z.; Shi, H.; He, X. X.; Wang, K. M.; He, D. G.; Guo, Q. P.; Qing, Z. H.; Yan, L. A.; Ye, X. S.; Li, D.; Tang, J. L. *Anal. Chem.*, 2014, **86**, 6976-6982.

28 Feng, X. B.; Gan, N.; Zhang, H. R.; Li, T. H.; Cao, Y. T.; Hu, F. T.; Jiang, Q. L. *Biosens. Bioelectron.*, 2016, **75**, 308-314.

29 Liao, Y. H.; Huang, R. Z.; Ma, K.; Wu, Y. X.; Zhou, X. M.; Xing, D. *Anal. Chem.,* 2014, **86**, 4596-4604.

30 Tian, T.; Xiao, H.; Zhang, Z. G.; Long, Y. L.; Peng, S.; Wang, S. R.; Zhou, X.; Liu,

S. M.; Zhou, X. *Chem.-Eur. J.*, 2013, **19**, 92-95.

31 Wan, Z. Y.; Han, J. X.; Cui, Y. Z.; Zhou, X. Y.; Fan, K. X. *Biochem. Biph. Res. Co.*, 2013, **439**, 384-389.

32 Zhu, J.; Hu, X. Q.; Guo, G. L. and et al, *Chin. J. of Surg.*, 2010, **48**, 205-208.

33 Lu, Y. J.; Xiao, J. N.; Lin, H. X.; Bai, Y. L.; Luo, X. B.; Wang, Z. G.; Yang, B. F. *Nucleic Acids Res.*, 2009, **37**, 1-10.

for TOC only

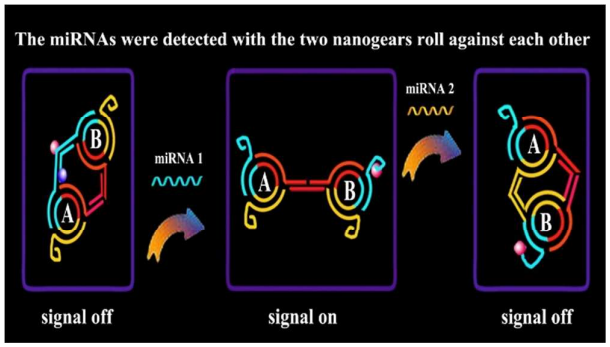
The miRNAs were detected with the two nanogears roll against each other
miRNA 1
miRNA 2
A
B
signal off
signal on
signal off